RESEARCH PAPER

A Novel Bacoside A–Loaded Thermoresponsive In Situ Hydrogel for Accelerated Acute Wound Healing

Dr. Dheeraj D. Chechare[1], Dr. Mahendra B. Datir[2], Dr. Vivekanand A. Kashid[3], Dr.Tejas Pachpute[4], Dr. Santosh S. Dengale[5], Dr. Bhagyashree R. Dhambore[6], Mr.Rushikesh K Salve[7]

[1]Assistant Professor, PRES's College of Pharmacy (D &B.Pharm), Nashik, Maharastra
[2] (Corresponding Author) Associate Professor & H OD. M.A.B.D. Institute of pharmaceutical Education and Research,
Nashik, Maharashtra
Email: datirmahi@rediffmail.com
[3]Principal, M.A.B.D. Institute of pharmaceutical Education and Research,
Nashik, Maharashtra
[4]Principal, Jaihind College of Pharmacy , Pune, Maharastra
[5]Professor and Principal, Dr. Naikwadi College of Pharmacy, Nashik, Maharashtra
[6]Associate Professor & H O D, Dr. Naikwadi, College of Pharmacy, Nashik, Maharashtra
[7]Assistant Professor, M.A.B.D. Institute of pharmaceutical Education and Research, Nashik, Maharashtra

ABSTRACT

Objectives: To design and strengthen a thermosensitive in-situ hydrogel containing Bacoside A for enhanced wound healing, focusing on optimal gelling characteristics, mucoadhesion, and antimicrobial efficacy. **Methods**: Statistical optimization was used to construct thermosensitive hydrogels out of Poloxamer 407 and xantham gum. The physicochemical properties, drug content, rheology, and mucoadhesion of the formulations were analyzed in depth. Response surface methodology optimized gelling temperature and mucoadhesive strength. Ex-vivo permeation studies were conducted, followed by stability assessment and antimicrobial evaluation contrary E. coli and S. aureus. **Results**: The optimized formulation (RF6) exhibited ideal gelling temperature (33.78±0.78°C), mucoadhesive strength (2989.5±0.284 dyne/cm²), and viscosity (3185±0.923 cps). The statistical model showed high predictability (R^2>0.999) for both responses. Drug dispersion was persistent in ex vivo experiments, with 96.67±0.88% penetration at a flow of 11.59 µg/cm²/h and 8 hours. The formulation showed significant antibacterial activity with domains of restraint of 24.3±0.62 mm (E. coli) and 23.8±1.06 mm (S. aureus), comparable to the marketed standard. Product integrity was validated by stability studies over a six-month period with little variance in pertinent parameters. **Conclusion**: A potential substitute for traditional wound healing formulations, the established Bacoside A thermosensitive in situ hydrogel boasts intriguing qualities for wound healing applications by combining optimal gelling properties, sustained drug release, and significant antimicrobial activity.

Keywords: Bacoside A, Thermosensitive hydrogel, In-situ gelling, Wound healing, Response surface methodology, antimicrobial activity.

How to cite this article: Chechare DD, Datir MB, Kashid VA, Pachpute T, Dhambore BR, Dengale SS. A Novel Bacoside A–Loaded Thermoresponsive In Situ Hydrogel for Accelerated Acute Wound Healing. Int J Drug Deliv Technol. 2026;16(39s): 44-64. DOI: 10.25258/ijddt.16.39s.8

INTRODUCTION

Acute wounds refer to sudden injuries that lead to disruption of the skin's integrity and function due to physical trauma, thermal injuries, incisions, or cuts [1]. While chronic wounds do not heal within a short period of time, acute wounds have a proper timeline, wherein their healing may take days to weeks depending on the wound class and the patient more than 11 million patients yearly, and infection state [2]. Nevertheless, hindrances such as slow healing or infections can greatly impact on the recovery process [3]. Based on the recent research, acute wounds, especially burn injuries, are present in

develops in 10%–15% of them [4]. Currently, burn injuries cause about 180 000 death annually, of which about 75% are due to wound sepsis [5]. Several interventions that are used in the treatment of of chronic wounds include antibiotics, antimicrobial dressings, and debridement, which has their inherent challenges [6]. Antibiotic resistance, inability to effectively manage biofilms and the absence of advanced drug delivery system create complications that lead to prolonged hospital stays and poor patient outcome thus a call for innovative approaches in managing acute Wound Care [7].

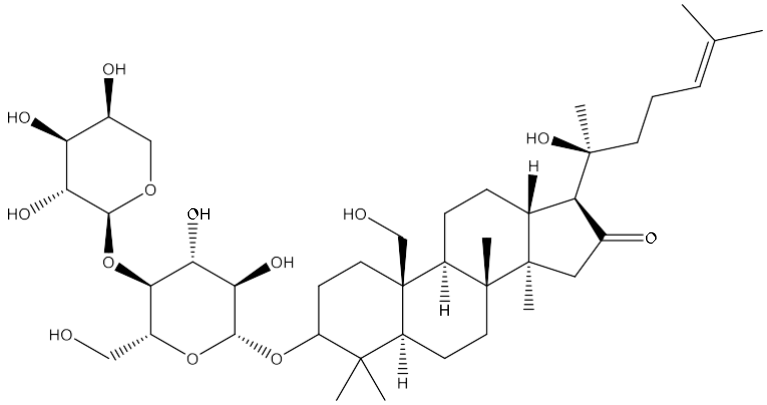

Figure 1: Chemical structure of Bacoside A

Bacoside A, a triterpenoid saponin, is the primary bioactive compound found in *Bacopa monnieri*, a traditional medicinal herb widely used in Ayurveda [8]. This herb, often referred to as "Brahmi," grows abundantly in wetlands and marshy areas, with its leaves being the richest source of Bacoside A [9]. famed for being a strong anti-inflammatory, antioxidant, and neuroprotective properties, In recent years, bacoside A has drawn particular intrigued out of its therapeutic potential in wound healing [10]. Studies suggest that Bacoside A can accelerate the wound-healing process by reducing oxidative stress, a major factor in delayed healing, and modulating inflammatory pathways [11]. It promotes the proliferation and migration of fibroblasts and keratinocytes, key cells involved in tissue regeneration [12]. Furthermore, Bacoside A's ability to combat microbial infections makes it a promising candidate for treating acute wounds, offering a dual action of promoting tissue repair while preventing infections [13].

Thermosensitive hydrogels are an advanced class of polymeric materials that exhibit a unique sol-to-gel transition in response to temperature changes [14]. At lower temperatures, these hydrogels remain in a liquid state, facilitating easy application over irregular wound surfaces [15]. Upon exposure to body temperature, they transition into a gel-like state, forming a stable, protective barrier over the wound [16]. Maintaining a moist wound environment is an essential part of helping wounds heal faster and more effectively, and this barrier does just that. [17]. Moreover, thermosensitive hydrogels can be engineered to act as carriers for bioactive compounds like Bacoside A, letting restricted and long persisting evacuation of the therapeutic medicine directly at the wound site. This localized drug delivery enhances efficacy, and minimizes systemic side effects, making thermosensitive hydrogels a promising platform for acute wound treatment [18].

The study is meant to create and enhance a thermosensitive hydrogel incorporating Bacoside A for improving acute wound healing. By leveraging the synergistic properties of Bacoside A and thermosensitive hydrogels, this formulation seeks to offer a novel therapeutic approach that accelerates wound healing, reduces infection risks, and minimizes the need for frequent dressing changes. The ultimate goal is to provide a patient-friendly, effective solution that bridges the gaps in existing treatment modalities and significantly improves clinical outcomes.

MATERIALS AND METHODS

Materials

Research Lab Fine Chem Industries (Mumbai, India) provided the poloxamer 407, while Sciquaint Innovations (Pune, India) provided the bacoside A. The source of xanthan gum was Indianjadibuti, located in Delhi, India. Every other chemical and solvent used in the course of the experiment was of analytical quality.

Methods

Calibration curve of Bacoside A

Spectroscopic analysis of Bacoside A was performed using methanol as the solvent. A 10 mg sample of Bacoside A was dissolved in methanol in a 100 ml volumetric flask, forming a 100 µg/ml stock solution. Aliquots of this solution (1.0 to 6.0 ml) had been squeezed into varying 10 ml volumetric flasks and dispersed with methanol to create working standard solutions at concentrations of 10 to 60 µg/ml. A Shimadzu UV1900 spectrophotometer had been employed to monitor absorbance at 227 nm.[19]

Solubility Study

Bacoside A's peak solubility was evaluated in an array of solvents, including water, methanol, ethanol, phosphate buffer (pH 6.8), and DMSO. Excess drug was introduced into 50 mL each of the

solvents in 100 mL volumetric flasks, sealed, and subjected to orbital shaking at 50 rpm and 37 ± 0.5°C for 48 hours. Samples were clarified, diluted, and verified for absorbance at 227 nm using a UV-visible spectrophotometer after they had been adjusted for equilibrium. Absorbance values were then converted to concentration based on standard curves for each solvent. [20].

FTIR Spectroscopy

FTIR-8400S spectrophotometers were put to use to generate FTIR spectra of the pure drug. A 1:100 mixture of the drug and KBr powder was combined, ground, and compressed into a pellet for one minute using 15 tons of hydraulic pressure. After releasing pressure by rotating the side valve anticlockwise, the pellet was inserted into the sample holder. Scanning was done in the vicinity of 4000-400 cm-1,with a resolution of 4 cm-1 and a measured acceleration of 2 mm/sec. [21].

Differential Scanning Calorimetry

Differential scanning calorimetry (DSC) is recorded with a Perkin-Elmer Pyris-1 calorimeter (Osaka, Japan). Prior to analysis, the specimens had been warmed to remove any remaining moisture. In a 40 µL aluminum pan, roughly five micro grams of each sample was carefully balanced, assembled, and preserved. An empty pan containing alpha-alumina served as the reference. Thermal scans were obtained across a temperature assortment ranging from 50°C to 300°C at a combustion rate of 20°C/min under a perpetual nitrogen purge maintained at 20 mL/min.[22].

Dose selection for bacoside A

The dose of Bacoside A was selected based on previously reported efficacy studies by R. Sharath *et al* [24]. in rats, where 200 µg/mL demonstrated significant wound healing activity without any toxicity [23]. A method involving Km factors was used to convert the animal dosage to a human equivalent dose (HED) for the purposes of this investigation. 2.27 mg of Bacoside A for the formulation, or 0.03 mg/kg body weight, was the HED determined.

Experimental design for thermosensitive in-situ hydrogel.

A 32-full factorial design was implemented to boost the composition of thermosensitive hydrogel. The proportions of xanthan gum (B) and Poloxamer 407 (A) at the -1, 0, and +1 levels were the two separate, distinct variables. The levels of Poloxamer 407 (A) were 20%, 22.5%, and 25% w/w, and for Xanthan gum (B), 0.5%, 1.0%, and 1.5% w/w. The analyzed variables included sol-gel temperature (R1) and mucoadhesive strength (R2). According to the factorial design, 9 formulations were prepared. Experimental design was refined and verified with Design Expert software (version 13.0, Stat-Ease Inc.), with validation particulars provided in tables 1 and 2, which display both coded and real values of the independent factors in the factorial design. [25].

The equation for polynomials is:

$$Y = \beta_0 + \beta_1 X_1 + \beta_2 X_2 + \beta_{11} X_1^2 + \beta_{22} X_2^2 + \beta_{12} X_1 X_2 + \varepsilon \quad (1)$$

Y represents the replies variable, which can be R1 or R2. The model includes an intercept coefficient (β_0), linear effect coefficients (β_1, β_2), quadratic effect coefficients (β_{11}, β_{22}), an interaction effect coefficient (β_{12}), coded values of factors A (Poloxamer 407, X_1) and B (Xanthan Gum, X_2), as well as an error term (ε). [25].

Table 1: Encoded and actual levels employed in the 3^2 full factorial experimental design

Code	Factor Name	Coded Levels	Actual Concentration (% w/v)
A	Poloxamer 407	-1	0
B	Xanthan Gum	-1	0

Response (Dependent) Variables

R1: Gelation temperature (°C)

R2: Mucoadhesive strength (dyne/cm²)

Code	Formulation Component	Level (-1)	Level (0)	Level (+1)	Low Concentration (% w/v)	Medium Concentration (% w/v)	High Concentration (% w/v)

A	Poloxamer 407	-1	0	1	16	18	20
B	Xanthan Gum	-1	0	1	0.5	1	1.5

Reliant (Response) Variables

Code	Measured Response Parameter	Unit
R1	Gelation Temperature	°C
R2	Bioadhesive Force	Dyne/cm²

Table 2: Prepared batches of thermosensitive hydrogel using 3^2 factorial designs

Ingredients	F1	F2	F3	F4	F5	F6	F7	F8	F9
Bacoside A (mg)	2.27	2.27	2.27	2.27	2.27	2.27	2.27	2.27	2.27
Poloxamer 407 (% w/v)	16	18	20	16	18	20	16	18	20
Xanthan Gum (% w/v)	0.5	0.5	0.5	1.0	1.0	1.0	1.5	1.5	1.5
Distilled water (q.s)	q.s	q.s	q.s	q.s	q.s	q.s	q.s	q.s	q.s

Preparation of *In-situ* thermosensitive hydrogel

The hydrogel was prepared by cold method [26]. Weight of required grams of Poloxamer 407 and Xanthan gum were weighed, dissolved into ddH2O, heated to room temperature to 4 °C ± 0.5 °C overnight to make a sol solution of specified concentration (w/w). Clear solutions were obtained by dissolved polymers by stirring continuously at 40 rpm. Quantitative weighing of Bacoside A into ethanol solution was accomplished. Finally, a drug solution was then made by adding the drug solution into the polymeric solution at 40 rpm while stirring continuously until the medication concentration (itaconic acid) reaches 2.27 mg. Next, the hydrogel composite's thermosensitive traits were assessed. [27].

Evaluation of In-situ thermosensitive hydrogel

Gelling temperature

The vial flipping tactic was employed to discover the gelation temperature of thermosensitive hydrogels by heating samples in a water bath at 1°C per minute. By tilting the vials, the sol-to-gel transition could be seen, and the gelation temperature had been adjusted to the temperature at which the hydrogel stopped flowing. This method provides accurate assessment of phase transition under physiological conditions. [28].

Gelling time

By employing the vial inversion method, the time necessary for gelling was determined. [29]. The formulation was placed in a vial with a 2mL volume of the formulation and heated at a controlled temperature increment. The vial was periodically tilted to track the sol-gel evolution. The gelling time was recorded as the point when the formulation ceased flowing upon tilting.

Viscosity

By employing an S-94 spindle and a Brookfield viscometer, the in situ thermosensitive hydrogels' texture was assessed. The spindle penetrated perpendicularly into the gel and transferred prepared gel formulations into a beaker. Measurements were carried out at the speed of 100 rpm, the temperature being set 37± 0.5 °C. Viscosities of the formulations were measured while cooling and the measurements were done in triplicate to insure reliability and also accuracy [30].

Drug Content Assay

The in situ thermosensitive hydrogel formulation was diluted to a total volume of 10 mL with methanol and 1 mL was used to determine the drug content of the hydrogel. After vortexing the mixture to ensure complete dissolution, it was filtered to eliminate undissolved particles. A Shimadzu UV-1900 spectrophotometer was used to detect the absorbance of Bacoside A at 227 nm on the filtration stage. The illicit substance concentration was ascertained by comparing the transpiration values to a calibration curve using methanol. Finally all

measurements were done in triplicate to verify precision and reproducibility [31].

Mucoadhesive strength

To evaluate the in-situ thermosensitive gel's mucoadhesive strength, a modified physical balance method was employed. This involved attaching freshly excised mucosal tissue to two glass vials, one on a balance and the other on an adjustable platform. After applying a predetermined amount of gel to the mucosa in the first vial, the second vial was brought into close contact with the first, keeping it there for two minutes. The two vials were then weighed on the balance pan, gradually adding weights until the vials thus separated. The calculus was employed for estimating the mucoadhesive strength.[32]:

$$\text{Mucoadhesive strenghth} = \frac{m - g}{A}$$

Precise measurement of the gel's adhesive properties is made possible by this methodology, A is the mucosa's contact vicinity (measured in cm2), g is the gravitational constant (980 cm/s2), and m is the weight (in grams) needed to separate the vials.

Spreadability

To test a 5 g sample of thermosensitive hydrogel's spreadability, a 500 g mass was continuously pressed across two glass plates for five minutes. A calliper was used to measure the gel spread's diameter, and the test was run three times to guarantee accurate findings. The spreadability of the gel was measured to determine the diameter, at which the gel had spread, measured by a calliper. In this study, this test was done in triplicate to establish a reliable and consistent results [33].

Ex-vivo drug release study

An in vitro biological dispersion investigation relied on the goat skin as a diffusion membrane. It was obtained from a slaughterhouse and positioned between the donor and agonist compartments, with the agonist side having phosphate buffer at pH 6.8 and the donor side having 1 g of thermosensitive hydrogel. The went on at 37±0.5 °C and spun at 100 rpm. To determine the cumulative release percentage over time, 1 ml samples were taken out at regular intervals over the course of 8 hours, diluted with 10 ml of buffer, and spectroscopically measured at 227 nm. [34].

In-vitro antibacterial efficiency

Candiderma Plus, Bacoside A, and RF6 hydrogel had evaluated for their antibacterial activity against S. aureus and E. coli using the agar proficient diffusion technique. An E. Coli and S. aureus standardized bacterial solution was used to inoculate nutrient agar plates. A cork borer with a 6mm diameter was used to create the wells aseptically after the liquid inoculation media had completely solidified. Carefully placed extract and gel solution in each of these plates. Plates were left for 30 minutes to pre-diffusion. Following the plates' normalization to room temperature, they were incubated for 24 hours at 37ºC to check for microorganisms. The millimeters of the surrounding portions of restraint for each well were tracked and recorded. The research approach was executed three times, and outcomes were portrayed as mean ± standard deviation. [35].

Stability studies

The stability assessment of the thermoresponsive hydrogel formulation followed ICH Q1A (R2) guidelines more than 6 months, stored at 25 ± 2 °C and 60 ± 5% RH. Evaluations at 0, 3, and 6 months included analysis of physical characteristics, pH, chemical concentration, rheological behaviour, gelation temperature, mucoadhesive strength, and ex vivo drug permeation profile. [36,37].

Statistical Analysis

In order to assess the impact of unforeseen variables, Design-Expert® software (version 13.0) with a response surface approach was used to analyze the study data. To ascertain the statistical significance of the model terms, an ANOVA was performed. The formulation was optimized via desirability function analysis, focusing on target criteria for viscosity and spread ability.

RESULTS

Calibration curve of Bacoside A

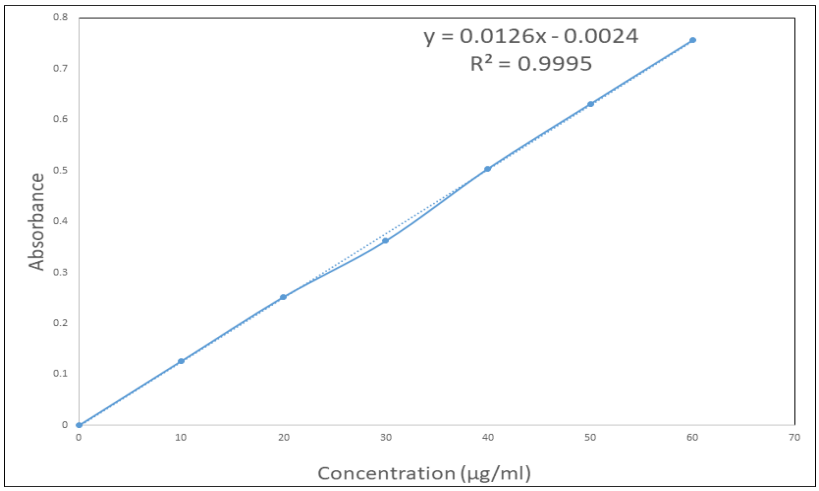

Figure 2: Standard Calibration Plot of Bacoside A in Methanol (λmax = 227nm)

Results of solubility study

Table 3: Equilibrium Solubility Profile of Bacoside A in Different Solvent Systems

S. No.	Medium / Solvent System	Observed Liquidity (mg/mL)*	Liquidity Recognition
1	Purified Water	2.57 ± 0.03	Tangibly unable to dissolve
2	Ethyl Alcohol	24.42 ± 2.56	Sparingly soluble
3	Methyl Alcohol	27.36 ± 1.23	Sparingly soluble
4	Phosphate Buffer Solution (pH 6.8)	42.32 ± 3.82	Soluble
5	Dimethyl Sulfoxide (DMSO)	76.98 ± 4.22	Soluble

Three measurements were acquired for each measurement, and the average values and standard deviations are shown.

Results of FTIR analysis

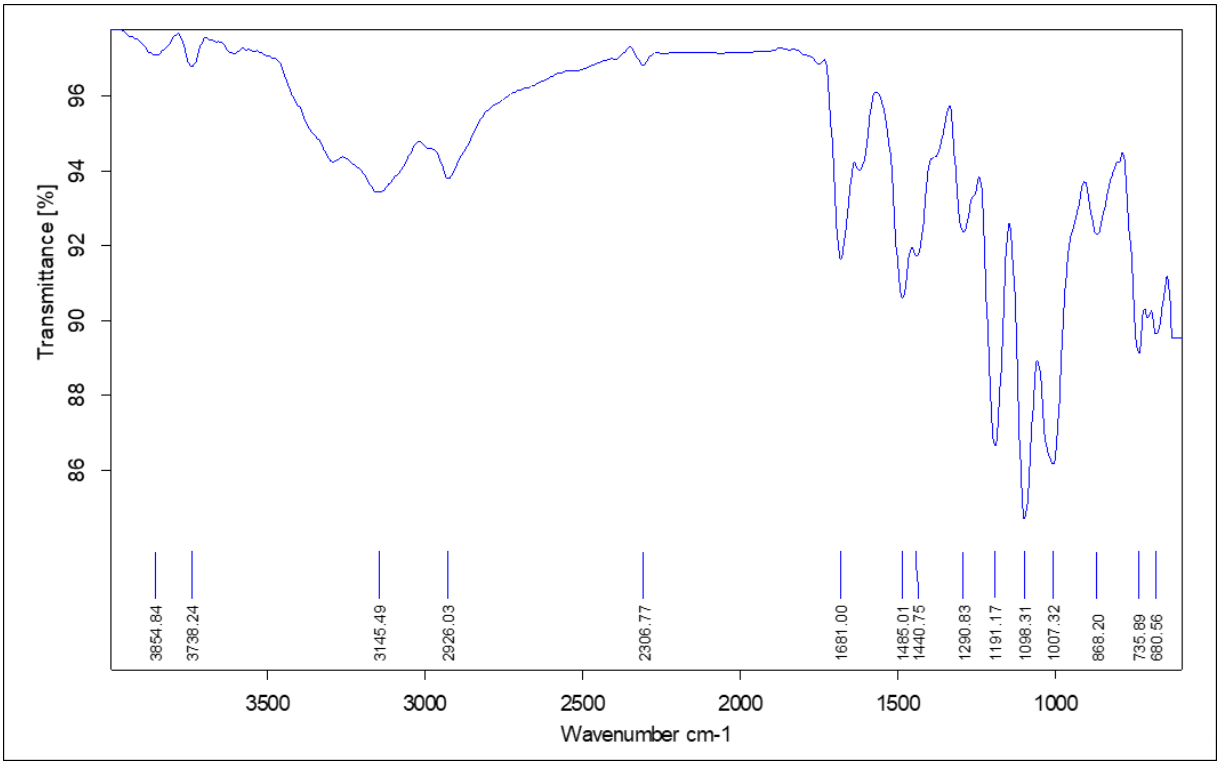

Figure 3: FTIR Spectral analysis of pure Bacoside A

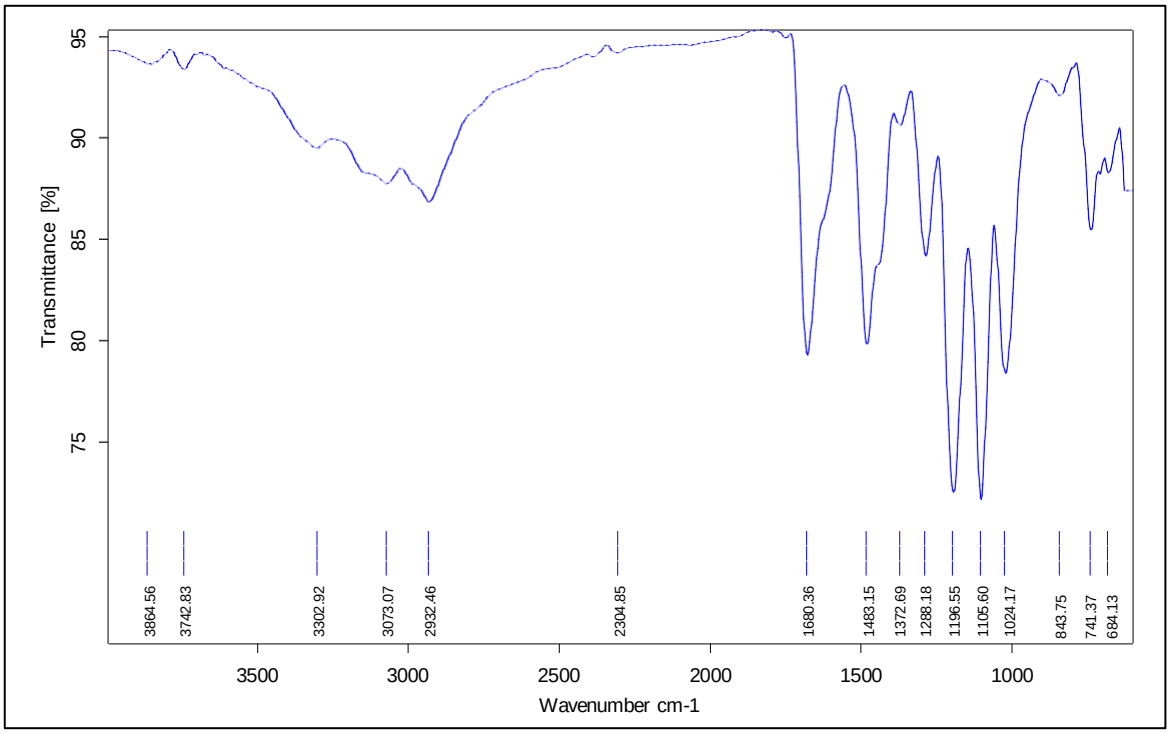

Figure 4: FTIR Spectral analysis of drug-excipient physical mixture

Results of differential Scanning Calorimetry

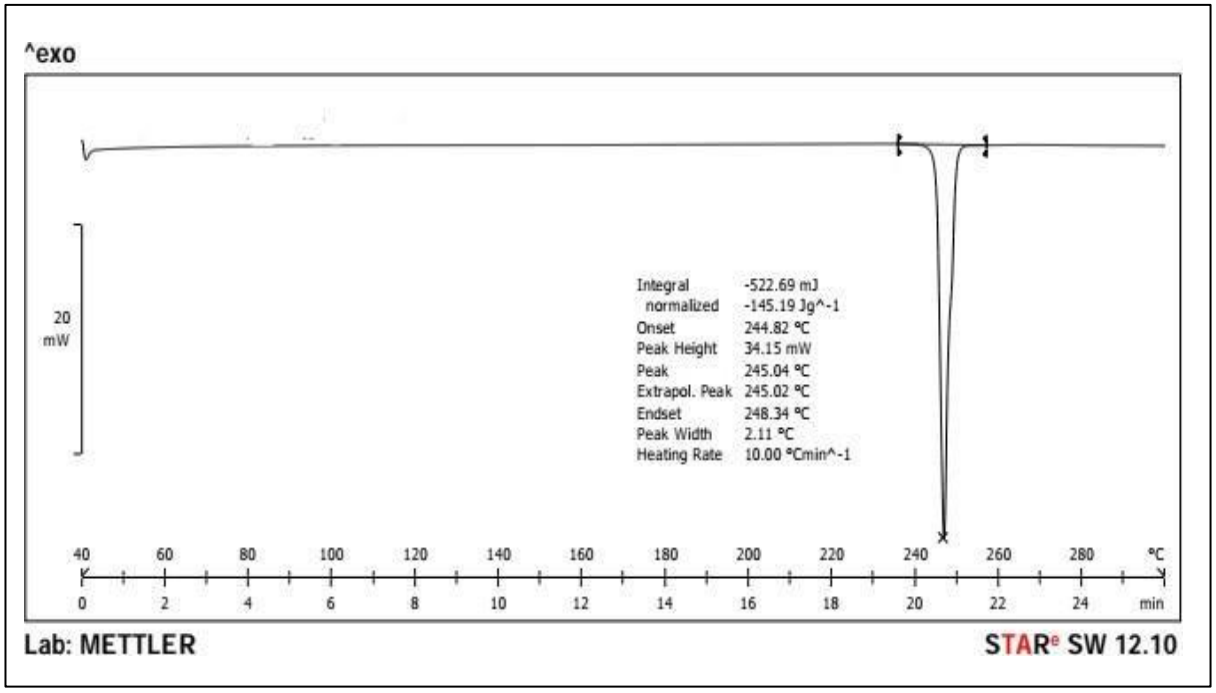

Figure 5: DSC thermogram of pure Bacoside A

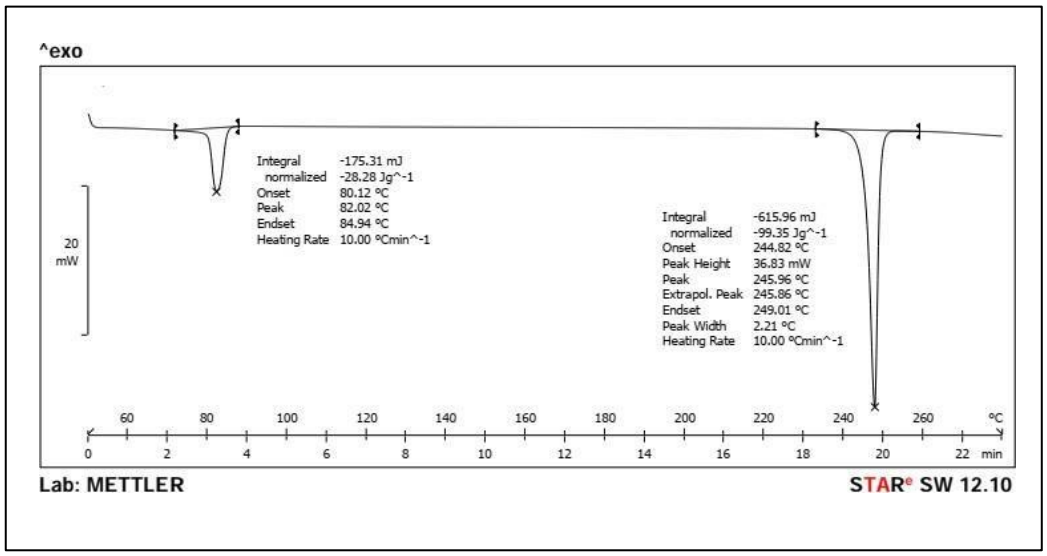

Figure 6: DSC Thermogram of drug-excipient Physical mixture

Characterization of thermosensitive in-situ hydrogel

Table 4: Assessment of Key Physicochemical Attributes Thermally sensitive in situ hydrogels

Experimental composition	Gelling temperature (°C)	Gelling time (sec)	Viscosity (cps)
RF1	43.23±0.28	37.34±0.12	2125±30
RF2	36.49±0.24	36.89±0.14	2532±26
RF3	32.8±0.20	37.64±0.10	2947±34
RF4	42.44±0.31	33.26±0.18	2280±29
RF5	36.45±0.26	32.72±0.15	2704±52
RF6	33.44±0.21	33.11±0.20	3105±40
RF7	42.96±0.34	30.1±0.17	2450±46

RF8	36.71±0.19	29.97±0.12	2885±30
RF9	32.87±0.30	30.19±0.16	3196±58

Values are stated as the average ± SD of three independent measurements (n = 3).

Table 5: Metrics for Thermosensitive In Situ Gel System Evaluation.

Experimental composition	Mucoadhesive strength (dyne/cm^2)	Drug content (%)	Spreadability (cm)
RF1	1798.9±0.415	91.7±0.49	8.1±0.26
RF2	1842.2±0.383	92.8±0.75	7.2±0.42
RF3	2039.8±0.744	90.3±0.40	11.3±0.51
RF4	2641.8±0.512	93.4±0.82	9.2±0.19
RF5	2838.6±0.483	92.9±0.63	12.1±0.68
RF6	2989.4±0.812	92.7±0.72	10.4±0.32
RF7	4278.2±0.641	91.4±0.94	11.5±0.83
RF8	4369.7±0.390	91.7±0.62	9.4±0.76
RF9	4539.1±0.673	92.6±0.47	8.8±0.82

The mean and associated standard deviation (n = 3) are portrayed by the values.

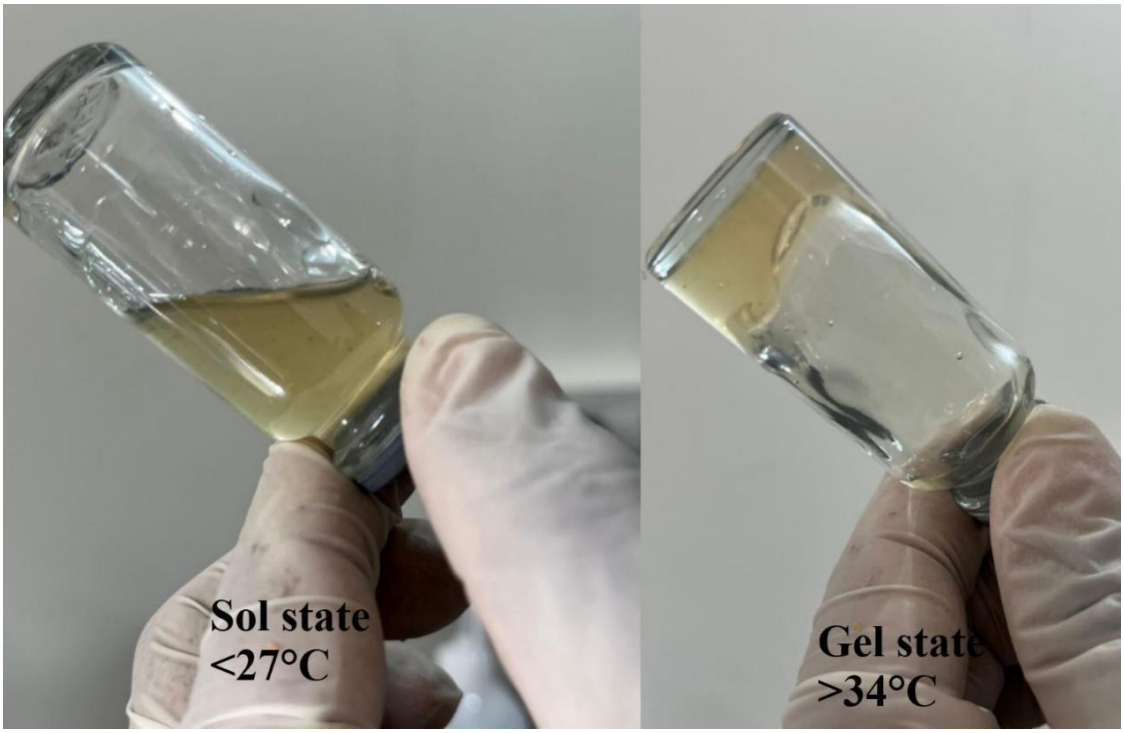

Figure 7: Image represents thermosensitive behavior of *in-situ* hydrogel in room temperature and physiological conditions.

Optimization of thermosensitive in-situ hydrogel

Effect of Independent variables on for gelling temperature (R_1)

Table 6: ANOVA Summary of the Second-Order Simulation for Gelling Warmth Response (R1)

Variation Source	SS (Sum of Squares)	DOF	MS (Mean Square)	F-Ratio	Probability (p)	Statistical Remark

Regression Model	149.23	5	29.85	157.01	0.0008	Meaningful
Factor A (Poloxamer 407)	145.24	1	145.24	764.04	0.0001	Meaningful
Factor B (Xanthan Gum)	0.0001	1	0.0001	0.0004	0.9862	Trivial difference
Interaction (A × B)	0.0289	1	0.0289	0.152	0.7226	Trivial difference
Quadratic Term (A^2)	3.96	1	3.96	20.82	0.0197	Trivial difference
Quadratic Term (B^2)	0.0089	1	0.0089	0.0468	0.8427	Trivial difference
Residual Inaccuracy	0.5703	3	0.1901	—	—	—
Rectified Sum	149.8	8	—	—	—	—

The mathematical relationship describing the influence of design attributes on cohesiveness temperature is expressed as follows:

Gelling Temperature=36.51−4.92*+0.0033*+0.0850 AB+1.24A^2+0.0667B^2 (1)

Where:

- **A** represents concentration of Poloxamer 407
- **B** represents concentration of Xanthan Gum
- **AB** denotes the interaction effect between factors
- **A^2 and B^2** indicate quadratic contributions of respective variables

Analysis of variance confirmed that the quadratic model was analytically noteworthy ($p < 0.05$), indicating a trustworthy connection between gelling warmth and unrelated variables. Among the tested factors, Poloxamer 407 exhibited a highly significant effect, whereas Xanthan gum showed no statistically significant linear influence. Poloxamer 407's diagonal segment was significant, indicating curvature in the response surface, whereas Xanthan gum's interaction term and diagonal segment were not statistically noteworthy.

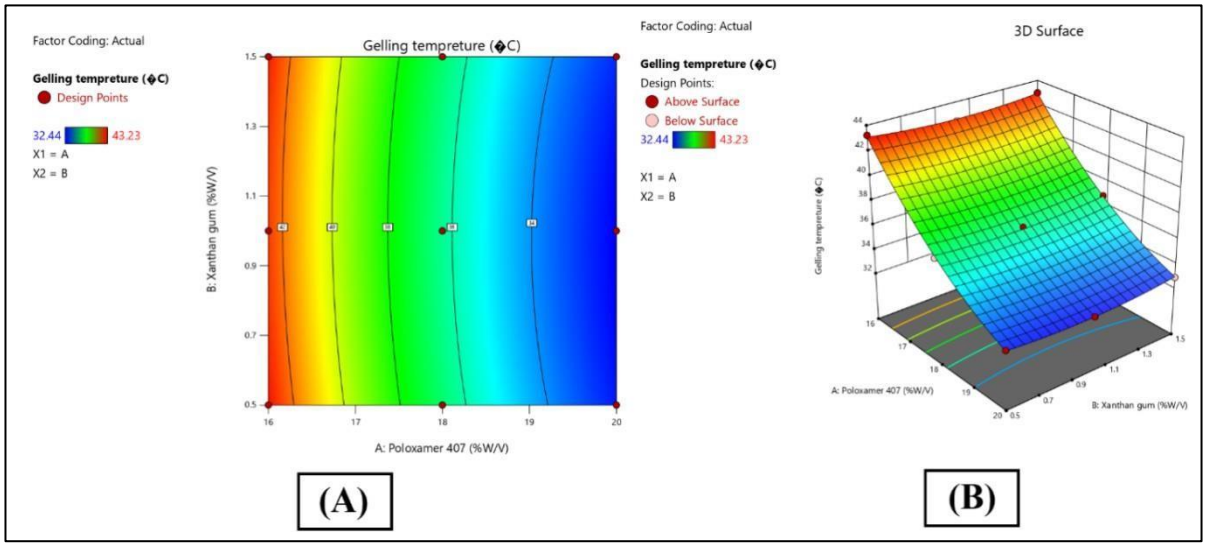

Figure 8: Contour plot (A) and 3D plot (B) of the effect of Poloxamer 407 and xanthan gum on the gelling temperature (R1) of an in-situ thermosensitive gel.

Response Surface Analysis of Variables Affecting Mucoadhesive Strength (R2)

Table 7: Statistical Summary (ANOVA) of the Diagonal Regression Simulation for Mucoadhesive Strength (R2)

Ancestor	Sum of Squares	df	Mean Square	F-value	p-value	
Simulation	9.719E+06	5	1.944E+06	893.99	< 0.0001	significant
A-Poloxamer 407	1.202E+05	1	1.202E+05	55.30	0.0050	
B-Xanthan gum	9.390E+06	1	9.390E+06	4318.70	< 0.0001	
AB	100.00	1	100.00	0.0460	0.8439	
A^2	1926.14	1	1926.14	0.8859	0.4160	
B^2	2.066E+05	1	2.066E+05	95.01	0.0023	
Residual	6522.98	3	2174.33			
Cor Total	9.726E+06	8				

Based on the derived polynomial exponential regression model, the mucoadhesive strength (R2) can be portrayed by the quadratic equation that ensues:

$$\text{Mucoadhesive strength} = +2802.58 + 141.57*A + 1251.02*B + 5.00*AB + 31.03*A^2 + 321.38*B^2 \quad (2)$$

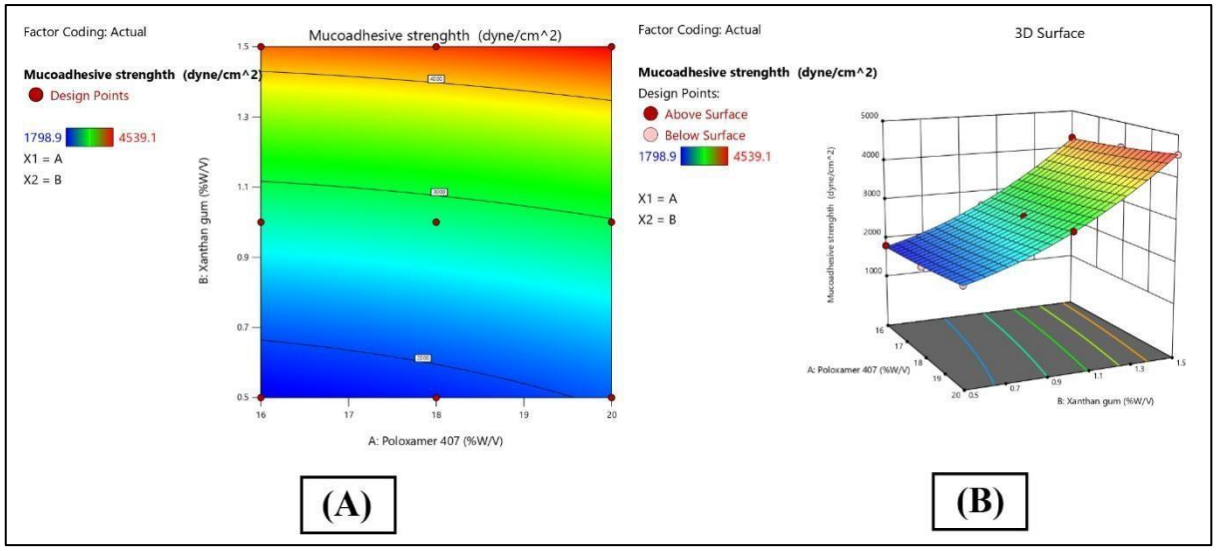

Figure 9: Contour (2D) and response surface (3D) representations showing the joint effect of Poloxamer 407 and xanthan gum on the mucoadhesive strength (R2) of the thermosensitive in situ gel.

Table 8. Analysis of quadratic model fitting parameters for gelling temperature (R1) and mucoadhesive strength (R2).

Diagonal Simulation	R^2	Adjusted R^2	Predicted R^2	SD	% CV
Respondent (R1)	0.9992	0.998	0.9927	0.1993	0.5332
Respondent (R2)	0.9993	0.9982	0.9932	46.63	1.54

Validation of statistical model

Table 9 shows the response variables' experimental and predicted values along with the proportional incorrectness.

F. Code	Composition	Actual (mg)	Response	Predicted value	Experimental value	Relative Error (%)
MF6	Poloxamer 407	20	Gelling temperature (°C)	34.01	34.44	1.26
	Xanthan gum	1				

MF6	Poloxamer 407	20	Mucoadhesive strength (dyne/cm^2)	3000	2989	0.37
	Xanthan gum	1				

Ex-vivo drug permeation study

Figure 8 displays the findings of studies on drug permeation conducted ex vivo.

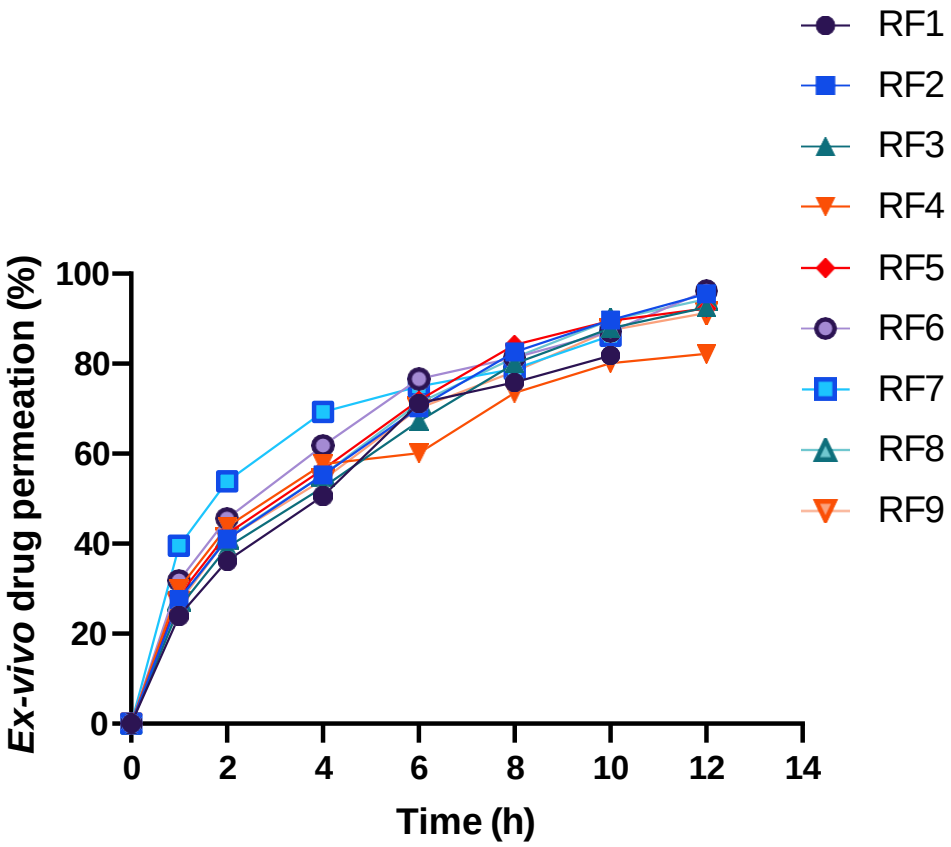

Figure 10: *Ex-vivo* drug permeation from *In-situ* thermosensitive hydrogel

Flux and Kp of thermosensitive hydrogel (RF1-RF9)

Table 10: Flux and Kp of thermosensitive hydrogel (RF1-RF9)

Batch Code	Mobility Flux (µg/cm²/h)	Seeming Permeability Coefficient Kp (cm/h)
RF1	10.90	1.090
RF2	10.66	1.066
RF3	10.24	1.024
RF4	9.09	0.909
RF5	10.89	1.089
RF6	11.59	1.159
RF7	11.05	1.105
RF8	10.82	1.082
RF9	10.63	1.063

Stability study

Table 11: Six-Month Stability Evaluation of Optimized Formulation Stored at 25 ± 2°C / 60 ± 5% RH

Evaluation Parameter	Initial (0 Month)	After 1 Month	After 3 Months	After 6 Months

Physical Clarity	Uniform and clear	Uniform and clear	Uniform and clear	Uniform and clear
Visual appearance	Unimpeded	Unimpeded	Unimpeded	Unimpeded
Gelation Temperature (°C)	33.78 ± 0.78	33.54 ± 0.67	33.48 ± 0.73	32.54 ± 0.83
Viscosity (cP)	3185 ± 0.923	3151 ± 0.645	3123 ± 0.482	3117 ± 0.787
Mucoadhesive Force (dyne/cm²)	2989.5 ± 0.284	2997.8 ± 0.833	3002.3 ± 0.156	3011.9 ± 0.723
Gelation Time (seconds)	21.4 ± 0.5	21.9 ± 0.6	21.4 ± 0.4	20.9 ± 0.3
pH	6.2 ± 0.07	6.2 ± 0.09	6.2 ± 0.03	6.2 ± 0.09
Spreadability (cm)	10.3 ± 0.43	10.8 ± 0.33	10.5 ± 0.93	10.8 ± 0.36
Drug permeation in ex vivo at 8 hours (%)	96.67 ± 0.88	96.63 ± 0.44	96.48 ± 0.73	94.41 ± 0.68

All values are presented as mean ± standard deviation (n = 3 independent measurements).

In-vitro antibacterial activity

Table 12: *In-vitro* antibacterial activity of Bacoside A, Thermosensitive hydrogel (RF6) and Candiderma Plus (Marketed standard).

S. No.	Test Formulation / Specimen	*Escherichia coli* (mm)	*Staphylococcus aureus* (mm)
1	Pure Bacoside A	26.9 ± 1.76	28.4 ± 0.38
2	Optimized Thermosensitive Hydrogel (RF6)	24.3 ± 0.62	23.8 ± 1.06
3	Commercial Preparation (Candiderma Plus)	29.3 ± 0.63	27.7 ± 0.19

Each value corresponds to the average ± standard deviation of three replicates.

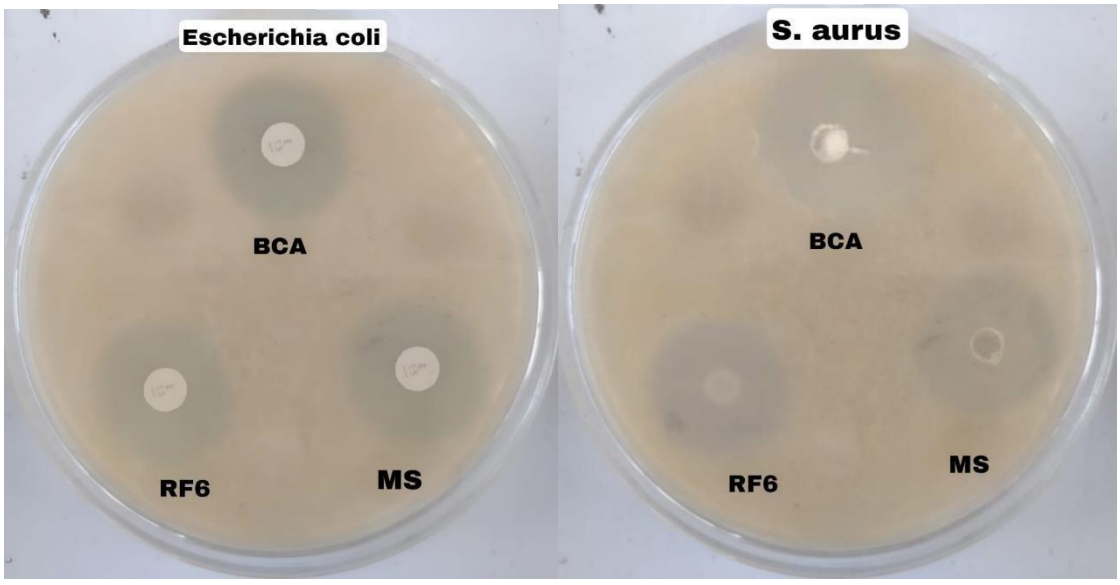

Figure 11: ***Assessment of the antibacterial efficacy of standard Candiderma Plus, RF6 thermogelling hydrogel, and pure Bacoside A against Staphylococcus aureus and Escherichia coli in vitro.***

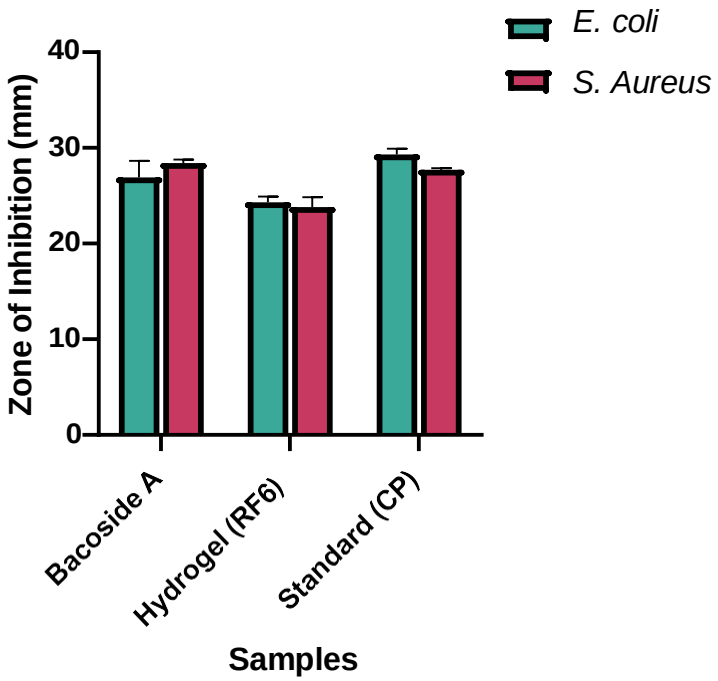

Figure 12: A representational illustration of Bacoside A, thermosensitive hydrogel (RF6), and Candiderma Plus (Standard) (MS)'s in vitro antibacterial activity against Staphylococcus aureus and Escherichia coli.

4. DISCUSSION

As illustrated in Figure 2, Bacoside A's calibration curve showed outstanding linearity with a correlation coefficient (R2) of 0.9995. A robust and consistent relationship between absorbance and concentration at 227 nm is shown by the linear regression equation (y = 0.0126x - 0.0024) [38]. This approach's precision and accuracy for interpreting Bacoside A in ulterior analyses are confirmed by this high R2 value, which makes it a reliable analytical tool for more formulation investigations. This spectrophotometric approach appears to be reliable and appropriate for routine measurement of Bacoside A in different formulation phases, as indicated by the linear response across the concentration range. [39].

Bacoside A's solubility analysis in various solvents, which is shown in Table 3, showed a clear solubility pattern that is essential for formulation development. DMSO exhibited the highest solubility (76.98±4.22 mg/mL), followed by phosphate buffer pH 6.8 (42.32±3.82 mg/mL), indicating these as preferred solvents for bacoside A incorporation [40]. The compound showed moderate solubility in alcoholic solvents, with methanol (27.36±1.23 mg/mL) and ethanol (24.42±2.56 mg/mL) demonstrating similar solubilizing capacity. The low water solubility of Bacoside A (2.57 ± 0.03 mg/mL) is noteworthy and emphasizes the necessity of using suitable solubility improvement techniques for creating the thermosensitive in situ hydrogel formulation. This solubility profile provides valuable insights for selecting suitable vehicles and developing effective formulation strategies to ensure optimal drug loading and release characteristics. [41].

As illustrated in Figures 3 and 4, the FTIR spectral detection of pure Bacoside A and its physical mixing with excipients revealed distinctive functional group peaks that shed light on the compatibility of the medicine with the excipient. O-H stretching (3854.84, 3738.24 cm^{-1}), N-H widens (3145.49 cm^{-1}), C-H stretching (2926.03 cm^{-1}), and other typical peaks belonging to different functional groups were all clearly visible in pure Bacoside A [42]. The majority of peaks, including O-H stretching (3864.56, 3742.83 cm^{-1}), N-H stretching (3302.92 cm^{-1}), and C-H stretching (2932.46 cm^{-1}), were retained with very minor alterations when compared to the physical mixture spectra. Although not substantial enough to prove incompatibility, the slight differences in peak positions and the lack of a C=C stretching peak in the physical combination point to certain molecular interactions. [43].

The DSC thermograms, shown in Figures 5 and 6, further substantiate the compatibility studies between Bacoside A and the excipients. Bacoside A pure showed a clear endothermic peak at 245.04°C

that represented its melting point. In the physical mixture thermogram, the characteristic peak of Bacoside A was retained at 245.96°C with minimal shift, indicating the drug's physical stability in the presence of excipients [44]. An additional endothermic peak observed at 82.02°C can be linked to the excipients' thermal behaviours in the tangible mixture. The preservation of Bacoside A's thermal profile in the mixture, with only slight peak modifications, suggests good compatibility between the drug and selected excipients, supporting their suitability for the formulation development [45].

As mentioned in Table 4, the physicochemical characterization of the thermosensitive *in-situ* hydrogel formulations also revealed differences in properties with regard to the formulated preparation. This reveals that the gelling temperature was from 32.8 °C and 43.23 °C and formulations with the closest optimal gelling temperature to that of physiological standard (32.8 ± 0.20 °C and 32.87 ± 0.30 °C) are formulation RF3 and RF9 respectively as shown in the figure 7 above. The gel formed a few seconds subsequent to execution for all formulations, with gelling times spanning from 29.97 to 37.64 seconds. The flow consistency/viscosity was determined to increase from RF1 to RF9 (2125±30 to 3196±58 cps) and it was established that the higher polymer concentrations increased viscosity which is important in order to hold gel structure at the area of application.

As it is seen in Table 5 below, there were noticeable differences in the test results of mucoadhesive strength, drug content, and film spreadability. It was observed that mucoadhesive strength values increased gradually up to RF9 (1798.9 ± 0.415 to 4539.1 ± 0.673 dyne/cm²), moreover, formulations RF7, RF8 and RF9 exhibited significantly greater mucoadhesive properties, which are especially important as would provide more time to product to remain at the healing site. recoveries were also fairly constant for all formulations in the range of 90.3-93.4% reflecting that the drug has disbursed evenly and the method of preparation of the formulation is effective [46]. The spreadability was numerically between 7.2±0.42 to 12.1±0.68 cm which in turn means that the formulation was easily applied on the buccal mucosa d/t to the drug's spread ability; the result was high for RF5 hence exhibiting good drug distribution. These parameters taken as a whole suggest that formulations RF3 and RF9 show the most favorable tendency for the wound healing application due to the optimal gelling temperature, moderate viscosity and adhesive properties to mucous membranes [47].

The optimization of thermosensitive *in-situ* hydrogel through ANOVA analysis for gelling temperature (R1), as shown in Table 6, reveals significant insights into the formulation variables' effects. The model demonstrated high statistical significance (F-value = 157.01, p-value = 0.0008), indicating its reliability in predicting gelling temperature [48]. Among the independent variables, Poloxamer 407 (A) emerged as the almost all influential attribute with an exceptionally high F-value (764.04) and significant p-value (0.0001), demonstrating its dominant role in controlling the gelling temperature of the formulation. This is further supported by its large sum of squares value (145.24), indicating that changes in Poloxamer 407 concentration account for the majority of variation in gelling temperature [48].

The quadratic regression equation and response surface plots (Figure 8) provide deeper insights into the relationship between variables and gelling temperature. The negative coefficient of A (-4.92) in the equation indicates that increasing Poloxamer 407 concentration leads to a decrease in gelling temperature, which is visually represented in both contour and 3D plots [49]. Interestingly, xanthan gum (B) showed minimal influence on gelling temperature, as evidenced by its negligible coefficient (0.0033) and non-significant p-value (0.9862). The correlation between segment (AB) and diagonal terms (A^2, B^2) had minimal impact, except for A^2 which showed significance (p=0.0197), a nonexistent hyperlink atwixt the extent of Poloxamer 407 and gelling temperature. The high model R^2 value implied by the small residual sum of squares (0.5703) indicates good fit and predictability of the model for optimizing gelling temperature in the formulation development [50].

The ANOVA analysis for mucoadhesive strength (R2), as presented in Table 7, reveals a highly significant model (F-value = 893.99, p-value < 0.0001), indicating excellent reliability in predicting mucoadhesive strength. In contrast to the gelling temperature results, xanthan gum (B) emerged as the dominant factor influencing mucoadhesive strength, with an exceptionally an elevated F-value (4318.70) and very valid p-value (< 0.0001). This is further evidenced by its substantial sum of squares value (9.390E+06), which represents the majority of the total variation in mucoadhesive strength. Poloxamer

407 (A) also showed significant influence (p=0.0050) but to a lesser extent than xanthan gum [51].

The relationship between variables and mucoadhesive strength, as measured by the regression equation, is depicted in Figure 9 using contour and 3D response surface plots. The large positive coefficient of xanthan gum (1251.02) in the equation demonstrates its strong positive correlation with mucoadhesive strength, as depicted by the ascending gradient in both plots. The quadratic term of xanthan gum (B^2) was also significant (p=0.0023), indicating a non-linear relationship with mucoadhesive strength. Interestingly, while Poloxamer 407 contributed positively to mucoadhesive strength (coefficient +141.57), its interaction with xanthan gum (AB) was negligible (p=0.8439), suggesting that both polymers independently contribute to the mucoadhesive properties. The contour plot (A) shows distinct color gradients from blue to red, clearly illustrating how increasing concentrations of both polymers, particularly xanthan gum, enhance mucoadhesive strength from 1798.9 to 4539.1 dyne/cm² [52].

The analytical validation of the optimization simulation, as presented in Table 8, demonstrates exceptional reliability and predictive capability for both responses. For gelling temperature (R1), the simulation showed excellent fit with very high R^2 (0.9992), adjusted R^2 (0.9980), and predicted R^2 (0.9927) values, indicating strong correlation between predicted and experimental values. Similarly, for mucoadhesive strength (R2), the model exhibited comparable robustness with R^2 (0.9993), adjusted R^2 (0.9982), and predicted R^2 (0.9932). The low coefficient of variation (CV%) values for both responses (0.5332% for R1 and 1.540% for R2) suggest high precision and reliability in the experimental data [53].

The correctness and dependability of the model are demonstrated by the validation of the optimized formulation (MF6). With a relative error of 1.26%, the experimental gelling temperature of 34.44°C was near the expected value of 34.01°C. With a low relative error of 0.37%, the mucoadhesive strength (2989 dyne/cm²) likewise matched the forecast (3000 dyne/cm²). These outcomes validate how well the optimization model predicts formulation responses. The low relative errors for both responses indicate that the developed mathematical model can reliably predict formulation characteristics, making it a valuable tool for optimizing thermosensitive in-situ hydrogel formulations [54].

The ex vivo drug permeation study, which is depicted in Figure 10, offers important information about how various thermosensitive in situ hydrogel formulations disperse drugs over a 12-hour period. All formulations reveal a biphasic pattern in the permeation profiles, with a swift release phase at the beginning and a sustained release phase at the end. In the first hour, formulation RF7 showed the highest initial drug permeation (39.46%), while other formulations exhibited lower initial release ranging from 23.98% to 31.75%. The quick dissolution is responsible for this initial burst release of surface-associated drug and the thermosensitive gel formation process [55].

The sustained release phase, observed from 2 to 12 hours, revealed varying permeation patterns among formulations. RF5 demonstrated optimal sustained release characteristics, achieving the highest cumulative drug permeation (96.21%) at 12 hours, followed closely by RF1 (95.51%) and RF6 (94.36%). The sustained release behavior can be attributed to the combined effect of Poloxamer 407's thermosensitive gelation and xanthan gum's matrix-forming properties. Notably, formulations RF3 and RF4 showed relatively lower cumulative permeation (82.2% and 92.32% respectively), suggesting that their polymer concentrations might have created a denser gel matrix, potentially limiting drug diffusion. The overall permeation profiles indicate that formulation RF5 achieves the optimal balance between initial release and sustained drug permeation, making it a viable option for applications involving wound healing requiring prolonged drug delivery [56].

The analysis of flux and permeability coefficient (Kp) values across formulations RF1-RF9, as shown in Table 10, reveals important insights into their drug permeation characteristics. Formulation RF6 demonstrated superior drug penetration, characterized by the highest permeability coefficient of 1.159 cm/h and a flux of 11.59 µg/cm²/h. This was followed closely by RF7 and RF1 with flux values of 11.05 and 10.90 µg/cm²/h respectively. Notably, RF4 showed the lowest flux (9.09 µg/cm²/h) and Kp (0.909 cm/h), suggesting that its polymer composition might have created a more restrictive barrier for drug diffusion. The relatively consistent flux values across most formulations (ranging from 10.24 to 11.59 µg/cm²/h) indicate that the polymer combinations generally provide controlled and predictable drug permeation [57].

The improved formulation's stability analysis, conducted over a six-month period at 25 ± 2°C/60 ± 5% RH, shows outstanding physical and chemical stability while maintaining transparency and clarity. There were only slight changes: the viscosity dropped from 3185±0.923 to 3117±0.787 cps, and the gelling temperature dropped from 33.78±0.78°C to 32.54±0.83°C. Interestingly, mucoadhesive strength showed a slight increase from 2989.5±0.284 to 3011.9±0.723 dyne/cm², possibly due to polymer chain reorganization. The formulation maintained consistent pH (6.2), spreadability (10.3-10.8 cm), and gelling time (20.9-21.9 sec). Over a six-month period, ex-vivo drug permeation at 8 hours decreased slightly from 96.67±0.88% to 94.41±0.68%, indicating strong drug stability and sustained release characteristics. These results collectively prove the structural and scientific durability of the optimized formulation under the tested storage conditions [58].

The *in-vitro* antibacterial activity assessment, as presented in Table 12 and illustrated in Figures 11 and 12, demonstrates significant antimicrobial efficacy of both pure Bacoside A and its thermosensitive hydrogel formulation (RF6) against both tested bacterial strains. Pure Bacoside A revealed substantial antibacterial effects, demonstrating restraint regions of 26.9±1.76 mm for E. coli and 28.4±0.38 mm for S. aureus, indicating its broad-spectrum antimicrobial potential. With inhibitory zones of 24.3±0.62 mm against E. coli and 23.8±1.06 mm against S. aureus, the thermosensitive hydrogel formulation (RF6) demonstrated strong antibacterial activity, but somewhat weaker than the pure medication. The economically available routine (Candiderma Plus) showed suppressive zones of 27.7±0.19 mm for S. aureus and 29.3±0.63 mm for E. coli, indicating similar efficacy to RF6. The hydrogel's controlled release feature, which modifies drug availability yet is advantageous for persistent curative impacts in wound healing exploits, is the cause of the decreased activity in comparison to pure Bacoside A and the standard. The comparable antibacterial activity profiles suggest that the developed thermosensitive hydrogel successfully preserves the antimicrobial properties of Bacoside A while providing the benefits of an in-situ gelling system, making it a viable substitute for traditional formulations for wound healing applications [59].

CONCLUSION

The completed and well-organized research on the development and refinement of Bacoside A loaded thermosensitive in-situ hydrogel discloses that the potential wound healing system can be formulated effectively. In optimized formulation, The gelling temperature, which was close to physiological temperature, was 33.78±0.78°C. After eight hours, the drug penetration efficiency was 96.67±0.88%, and the mucoadhesive strength was evaluated at 2989.5±0.284 dyne/cm². Signatures for conformation of compatibility of the drug-excipient interaction were established by FTIR and DSC In addition, optimization by RSM gave highly acceptable value of predictability of the designed formulation (R^2 > 0.999). The formulation proved to exhibit the best antibacterial efficacy against both the tested microbial isolates, and the result was as effective as a marketed lotion, though slightly inferior, and The study determined that the formulation demonstrated stability throughout a six-month investigation under the given storage conditions. The fact that the formulation is optimised with lasting drug release, mucoadhesion and their antimicrobial properties pointed to its potential use as an easy to apply, effective and comfortable to use *in-situ* thermosensitive hydrogel systemic medication for wound healing that has added benefits in comparison with conventional medication in terms of patient compliance.

Abbreviations

ANOVA, analysis of variance; DMSO, dimethyl sulfoxide; DSC, differential scanning calorimetry; FTIR, Fourier transform infrared spectroscopy; HPMC K4M, hydroxypropyl methylcellulose K4M; ICH, International Council for Harmonisation.

Acknowledgement

The authors express gratitude to the principal of SND College of Pharmacy, Yeola, for ongoing support and infrastructure, as well as to Sciquaint Innovations (OPC) Private Limited for supplying Bacoside A for their research.

Reference

[1] Bei Z, Zheng J. Recent advances in the application of functional hydrogels in skin wound healing. MedComm – Biomaterials and Applications 2024;3:e101. https://doi.org/10.1002/mba2.101.

[2] Falanga V, Isseroff RR, Soulika AM, Romanelli M, Margolis D, Kapp S, et al. Chronic wounds. Nature Reviews Disease Primers 2022;8:50.

[3] Monika P, Chandraprabha MN, Rangarajan A, Waiker PV, Chidambara Murthy KN. Challenges in healing wound: role of complementary and alternative medicine. Frontiers in Nutrition 2022;8:791899.

[4] Zhang P, Zou B, Liou Y-C, Huang C. The pathogenesis and diagnosis of sepsis post burn injury. Burns & Trauma 2021;9:tkaa047.

[5] Zhang P, Zou B, Liou Y-C, Huang C. The pathogenesis and diagnosis of sepsis post burn injury. Burns & Trauma 2021;9:tkaa047.

[6] Alves PJ, Barreto RT, Barrois BM, Gryson LG, Meaume S, Monstrey SJ. Update on the role of antiseptics in the management of chronic wounds with critical colonisation and/or biofilm. International Wound Journal 2021;18:342–58. https://doi.org/10.1111/iwj.13537.

[7] Kolimi P, Narala S, Nyavanandi D, Youssef AAA, Dudhipala N. Innovative treatment strategies to accelerate wound healing: trajectory and recent advancements. Cells 2022;11:2439.

[8] Murthy HN. Biotechnological production of bacosides from cell and organ cultures of Bacopa monnieri. Appl Microbiol Biotechnol 2022;106:1799–811. https://doi.org/10.1007/s00253-022-11834-0.

[9] Mondal S, Bhar K, Mondal P, Panigrahi N, Sahoo SK, Swetha P, et al. In quest of the mysterious holistic Vedic herb Bacopa monnieri (L.) Pennell. Pharmacognosy Research 2023;15.

[10] Nagori K, Nakhate KT, Yadav K, Ajazuddin, Pradhan M. Unlocking the Therapeutic Potential of Medicinal Plants for Alzheimer's Disease: Preclinical to Clinical Trial Insights. Future Pharmacology 2023;3:877–907.

[11] Martínez-Cuazitl A, Gómez-García M del C, Hidalgo-Alegria O, Flores OM, Núñez-Gastélum JA, Martínez ESM, et al. Characterization of polyphenolic compounds from bacopa procumbens and their effects on wound-healing process. Molecules 2022;27:6521.

[12] Martínez-Cuazitl A, Gómez-García M del C, Hidalgo-Alegria O, Flores OM, Núñez-Gastélum JA, Martínez ESM, et al. Characterization of polyphenolic compounds from bacopa procumbens and their effects on wound-healing process. Molecules 2022;27:6521.

[13] Ghosh D, Adhikary S, Bhattacherjee P, Debnath S. Herbal Medicine for Health Management and Disease Prevention. In: Izah SC, Ogwu MC, Akram M, editors. Herbal Medicine Phytochemistry, Cham: Springer International Publishing; 2024, p. 1–35. https://doi.org/10.1007/978-3-031-21973-3_31-1.

[14] Lacroce E, Rossi F. Polymer-based thermoresponsive hydrogels for controlled drug delivery. Expert Opinion on Drug Delivery 2022;19:1203–15. https://doi.org/10.1080/17425247.2022.2078806.

[15] Dong R, Guo B. Smart wound dressings for wound healing. Nano Today 2021;41:101290.

[16] Yu Y, Cheng Y, Tong J, Zhang L, Wei Y, Tian M. Recent advances in thermo-sensitive hydrogels for drug delivery. Journal of Materials Chemistry B 2021;9:2979–92.

[17] Nuutila K, Eriksson E. Moist Wound Healing with Commonly Available Dressings. Advances in Wound Care 2021;10:685–98. https://doi.org/10.1089/wound.2020.1232.

[18] Kolahreez D, Ghasemi-Mobarakeh L, Liebner F, Alihosseini F, Quartinello F, Guebitz GM, et al. Approaches to Control and Monitor Protease Levels in Chronic Wounds. Advanced Therapeutics 2024;7:2300396. https://doi.org/10.1002/adtp.202300396.

[19] Furukawa H, Ichimaru N, Suzuki K, Nishino M, Broughton J, Leinders J, et al. The comparative verification of calibration curve and background fundamental parameter methods for impurity analysis in drug materials. X-Ray Spectrometry 2017;46:382–7. https://doi.org/10.1002/xrs.2788.

[20] Mota FL, Carneiro AP, Queimada AJ, Pinho SP, Macedo EA. Temperature and solvent effects in the solubility of some pharmaceutical compounds: Measurements and modeling. European Journal of Pharmaceutical Sciences 2009;37:499–507.

[21] Ledeti I, Bolintineanu S, Vlase G, Circioban D, Ledeti A, Vlase T, et al. Compatibility study between antiparkinsonian drug Levodopa and excipients by FTIR spectroscopy, X-ray diffraction and thermal analysis. J Therm Anal Calorim 2017;130:433–41. https://doi.org/10.1007/s10973-017-6393-2.

[22] Rosasco MA, Bonafede SL, Faudone SN, Segall AI. Compatibility study of tobramycin and pharmaceutical excipients using differential scanning calorimetry, FTIR, DRX, and HPLC. J Therm Anal Calorim 2018;134:1929–41. https://doi.org/10.1007/s10973-018-7282-z.

[23] Sharath R, Harish BG, Krishna V, Sathyanarayana BN, Swamy HMK. Wound healing and protease inhibition activity of Bacoside-A, isolated from Bacopa monnieri wettest. Phytother Res 2010;24:1217–22. https://doi.org/10.1002/ptr.3115.

[24] Nair AB, Jacob S. A simple practice guide for dose conversion between animals and human. Journal of Basic and Clinical Pharmacy 2016;7:27.

[25] Jeswani G, Chablani L, Gupta U, Sahoo RK, Nakhate KT, Taksande AG. Exploration of hemocompatibility and intratumoral accumulation of paclitaxel after loco-regional administration of thermoresponsive hydrogel composed of poloxamer and xanthan gum: an application to dose-dense chemotherapy. International Journal of Biological Macromolecules 2023;226:746–59.

[26] Liang H-F, Hong M-H, Ho R-M, Chung C-K, Lin Y-H, Chen C-H, et al. Novel Method Using a Temperature-Sensitive Polymer (Methylcellulose) to Thermally Gel Aqueous Alginate as a pH-Sensitive Hydrogel. Biomacromolecules 2004;5:1917–25. https://doi.org/10.1021/bm049813w.

[27] Gao B, Luo J, Liu Y, Su S, Fu S, Yang X, et al. Intratumoral Administration of Thermosensitive Hydrogel Co-Loaded with Norcantharidin Nanoparticles and Doxorubicin for the Treatment of Hepatocellular Carcinoma. IJN 2021;Volume 16:4073–85. https://doi.org/10.2147/IJN.S308057.

[28] Nawaz A, Ullah S, Alnuwaiser MA, Rehman FU, Selim S, Al Jaouni SK, et al. Formulation and Evaluation of Chitosan-Gelatin Thermosensitive Hydrogels Containing 5FU-Alginate Nanoparticles for Skin Delivery. Gels 2022;8:537. https://doi.org/10.3390/gels8090537.

[29] Kolawole OM, Cook MT. In situ gelling drug delivery systems for topical drug delivery. European Journal of Pharmaceutics and Biopharmaceutics 2023;184:36–49. https://doi.org/10.1016/j.ejpb.2023.01.007.

[30] Srivastava R, Srivastava S, Singh SP. Thermoreversible in-situ nasal gel formulations and their pharmaceutical evaluation for the treatment of allergic rhinitis containing extracts of moringa olifera and embelia ribes. Int J Appl Pharm 2017;9:16.

[31] Fatouh AM, Elshafeey AH, Abdelbary A. Agomelatine-based *in situ* gels for brain targeting via the nasal route: statistical optimization, *in vitro* , and *in vivo* evaluation. Drug Delivery 2017;24:1077–85. https://doi.org/10.1080/10717544.2017.1357148.

[32] Permana AD, Utomo E, Pratama MR, Amir MuhN, Anjani QK, Mardikasari SA, et al. Bioadhesive-Thermosensitive *In Situ* Vaginal Gel of the Gel Flake-Solid Dispersion of Itraconazole for Enhanced Antifungal Activity in the Treatment of Vaginal Candidiasis. ACS Appl Mater Interfaces 2021;13:18128–41. https://doi.org/10.1021/acsami.1c03422.

[33] S. Mohamad SNF, Stephanie S, Sapiun Z, Tangdilintin F, Sulistiawati S, Himawan A, et al. Enhanced and Sustained Transdermal Delivery of Oxypurinol Using Thermosensitive Gel Combined with Polymeric Solid Microneedles. ACS Omega 2024:acsomega.4c07716. https://doi.org/10.1021/acsomega.4c07716.

[34] Bajwa M, Tabassam N, Hameed H, Irfan A, Zaman M, Khan MA, et al. Thermo-Responsive Sol-Gel-Based Nano-Carriers Containing Terbinafine HCl: Formulation, In Vitro and Ex Vivo Characterization, and Antifungal Activity. Gels 2023;9:830. https://doi.org/10.3390/gels9100830.

[35] Chavez-Esquivel G, Cervantes-Cuevas H, Ybieta-Olvera LF, Briones MC, Acosta D, Cabello J. Antimicrobial activity of graphite oxide doped with silver against Bacillus subtilis, Candida albicans, Escherichia coli, and Staphylococcus aureus by agar well diffusion test: Synthesis and characterization. Materials Science and Engineering: C 2021;123:111934.

[36] Bayanati M, Khosroshahi AG, Alvandi M, Mahboobian MM. Fabrication of a Thermosensitive In Situ Gel Nanoemulsion for Nose to Brain Delivery of Temozolomide. Journal of Nanomaterials 2021;2021:1546798. https://doi.org/10.1155/2021/1546798.

[37] Thermosensitive Brinzolamide in situ Gel Nanoemulsions, in vitro and ex vivo Evaluation. Biointerface Res Appl Chem 2020;11:7754–64. https://doi.org/10.33263/BRIAC111.77547764.

[38] Sabah R. Simultaneous HPLC estimation of Amphetamine and Caffeine abuse drugs in Iraqi human addicts. Journal of Advanced Sciences and Engineering Technologies 2021;4:25–31.

[39] Malviya V. Preparation and evaluation of emulsomes as a drug delivery system for bifonazole. Indian Journal of Pharmaceutical Education and Research 2021;55:86–94.

[40] Wali AF, Sridhar SB, Talath S, Pillai JR, Shareef J, Bhupathyraaj M, et al. Determination of the solubility of methyldopa in supercritical carbon dioxide for drug delivery applications: thermal analysis. Scientific Reports 2025;15:923.

[41] Das B, Baidya AT, Mathew AT, Yadav AK, Kumar R. Structural modification aimed for improving solubility of lead compounds in early phase drug discovery. Bioorganic & Medicinal Chemistry 2022;56:116614.

[42] Delbeck S, Heise HM. Systematic stability testing of insulins as representative biopharmaceuticals using ATR FTIR-spectroscopy with focus on quality assurance. Journal of Biomedical Optics 2021;26:043007–043007.

[43] Zhang Y, Chen J, Zhang Z, Zhu H, Ma W, Zhao X, et al. Solvent-Free Loading of Vitamin A Palmitate into β-Cyclodextrin Metal-Organic Frameworks for Stability Enhancement. AAPS PharmSciTech 2023;24:136. https://doi.org/10.1208/s12249-023-02596-7.

[44] Almoselhy R. Comparative study of vegetable oils oxidative stability using DSC and Rancimat methods. Egyptian Journal of Chemistry 2021;64:299–312.

[45] Nguyen HL, Bechtold T. Thermal stability of natural dye lakes from Canadian Goldenrod and onion peel as sustainable pigments. Journal of Cleaner Production 2021;315:128195.

[46] Hamzah ML, Kassab HJ, Alshahrani SM. Formulation and development of frovatriptan succinate in situ gel for nasal drug delivery: In vitro and ex vivo evaluation. Pakistan Journal of Pharmaceutical Sciences 2024;37.

[47] Joshi V, Kumar K, Negi A, Joshi A, Rajput V. World Journal of Current Medical and Pharmaceutical Research 2023.

[48] Polat HK, Arslan A, Ünal S, Haydar MK, Aytekin E, Gözcü S, et al. Formulation Development of Dual Drug-Loaded Thermosensitive Ocular In Situ Gel Using Factorial Design. J Pharm Innov 2023;18:768–88. https://doi.org/10.1007/s12247-023-09762-1.

[49] Mohapatra S, Mirza MA, Ahmad S, Farooq U, Ansari MJ, Kohli K, et al. Quality by design assisted optimization and risk assessment of black cohosh loaded ethosomal gel for menopause: Investigating different formulation and process variables. Pharmaceutics 2023;15:465.

[50] Ali AA, Hassan AH, Eissa EM, Aboud HM. Response Surface Optimization of Ultra-Elastic Nanovesicles Loaded with Deflazacort Tailored for Transdermal Delivery: Accentuated Bioavailability and Anti-Inflammatory Efficacy. IJN 2021;Volume 16:591–607. https://doi.org/10.2147/IJN.S276330.

[51] Nining N, Amalia A, Zahrok F. Response surface methodology for optimization of turmeric essential oil-loaded nanoemulgel. JRP 2023;27:1499–512.

[52] Barangule SP, Maru AD. Design and development of thermosensitive rectal in situ gel from Luffa acutangula fruits for the treatment of ulcerative colitis. Journal of Applied Pharmaceutical Research 2024;12:102–15.

[53] Shiehzadeh F, Mohebi D, Chavoshian O, Daneshmand S. Formulation, characterization, and optimization of a topical gel containing tranexamic acid to prevent superficial bleeding: In vivo and in vitro evaluations. Turkish Journal of Pharmaceutical Sciences 2023;20:261.

[54] Hirun N, Kraisit P, Tantishaiyakul V. Thermosensitive polymer blend composed of poloxamer 407, poloxamer 188 and polycarbophil for the use as mucoadhesive in situ gel. Polymers 2022;14:1836.

[55] Xu Y, Shrestha N, Préat V, Beloqui A. An overview of in vitro, ex vivo and in vivo models for studying the transport of drugs across intestinal barriers. Advanced Drug Delivery Reviews 2021;175:113795.

[56] Zhang Y, Dou X, Zhang L, Wang H, Zhang T, Bai R, et al. Facile fabrication of a biocompatible composite gel with sustained release of aspirin for bone regeneration. Bioactive Materials 2022;11:130–9.

[57] Anju K, Priya S, Sandeep DS, Nayak P, Kumar P, Kumar A, et al. Formulation and optimization of Zaltoprofen loaded ethosomal gel by using 23 full factorial designs. Journal of Pharmaceutical Research International 2021;33:30–44.

[58] Al Fatease A, Alqahtani A, Khan BA, Mohamed JMM, Farhana SA. Preparation and characterization of a curcumin nanoemulsion

gel for the effective treatment of mycoses. Scientific Reports 2023;13:22730.

[59] Saadon KE, Taha NMH, Mahmoud NA, Elhagali GAM, Ragab A. Synthesis, characterization, and in vitro antibacterial activity of some new pyridinone and pyrazole derivatives with some in silico ADME and molecular modeling study. J IRAN CHEM SOC 2022;19:3899–917. https://doi.org/10.1007/s13738-022-02575-y.